International Telecommunication Union

ITU-R

Radiocommunication Sector of ITU

Recommendation ITU-R M.1851

(06/2009)

Mathematical models for radiodetermination radar systems antenna patterns for use in interference analyses

M Series

Mobile, radiodetermination, amateur and related satellite services

Foreword

The role of the Radiocommunication Sector is to ensure the rational, equitable, efficient and economical use of the radio-frequency spectrum by all radiocommunication services, including satellite services, and carry out studies without limit of frequency range on the basis of which Recommendations are adopted.

The regulatory and policy functions of the Radiocommunication Sector are performed by World and Regional Radiocommunication Conferences and Radiocommunication Assemblies supported by Study Groups.

Policy on Intellectual Property Right (IPR)

ITU-R policy on IPR is described in the Common Patent Policy for ITU-T/ITU-R/ISO/IEC referenced in Annex 1 of Resolution ITU-R 1. Forms to be used for the submission of patent statements and licensing declarations by patent holders are available from http://www.itu.int/ITU-R/go/patents/en where the Guidelines for Implementation of the Common Patent Policy for ITU-T/ITU-R/ISO/IEC and the ITU-R patent information database can also be found.

Series of ITU-R Recommendations

(Also available online at http://www.itu.int/publ/R-REC/en)

Series	Title
BO	Satellite delivery
BR	Recording for production, archival and play-out; film for television
BS	Broadcasting service (sound)
BT	Broadcasting service (television)
F	Fixed service
M	**Mobile, radiodetermination, amateur and related satellite services**
P	Radiowave propagation
RA	Radio astronomy
RS	Remote sensing systems
S	Fixed-satellite service
SA	Space applications and meteorology
SF	Frequency sharing and coordination between fixed-satellite and fixed service systems
SM	Spectrum management
SNG	Satellite news gathering
TF	Time signals and frequency standards emissions
V	Vocabulary and related subjects

Note: *This ITU-R Recommendation was approved in English under the procedure detailed in Resolution ITU-R 1.*

Electronic Publication
Geneva, 2009

RECOMMENDATION ITU-R M.1851

Mathematical models for radiodetermination radar systems antenna patterns for use in interference analyses

(2009)

Scope

This Recommendation describes radiodetermination radar systems antenna patterns to be used for single-entry and aggregate interference analysis. Given knowledge about antenna 3 dB beamwidth and first peak side-lobe level, the proper set of equations for both azimuth and elevation patterns may be selected. Both peak, for single interferer, and average patterns, for multiple interferers, are defined.

The ITU Radiocommunication Assembly,

considering

a) that there is no defined antenna pattern equations for radiodetermination radar systems, within the ITU-R Recommendations, for use in interference assessments;

b) that a mathematical model is required for generalized patterns of antennas for interference analyses when no specific pattern is available for the radiodetermination radar systems,

recommends

1 that, if antenna patterns and/or pattern equations applicable to the radar(s) under study are available in other ITU-R Recommendations dealing with radiodetermination radar system characteristics, then those should be used;

2 that, in the absence of particular information concerning the antenna patterns of the radiodetermination radar system antenna involved, one of the mathematical reference antenna models described in Annex 1 may be used for interference analysis.

Annex 1

Mathematical models for radiodetermination radar systems antenna patterns for use in interference analyses

1 Introduction

A generalized mathematical model for radiodetermination radar systems antenna patterns is required when these patterns are not defined in ITU-R Recommendations applicable to the radiodetermination radar system under analysis. Generalized antenna pattern models could be used in analyses involving single and multiple interferer entries, such as that from other radar and communication systems.

This text describes proposed antenna patterns to be used. Given knowledge about beamwidth and the first peak side-lobe level, the proper set of equations for both azimuth and elevation patterns may be selected.

The result of surveyed antenna parameter ranges from ITU-R Recommendations are recorded in Table 1.

TABLE 1

Surveyed antenna parameter limits

Antenna parameter	Description	Minimum value	Maximum value
Transmit and receive frequencies (MHz)		420	33 400
Antenna polarization type	Horizontal, vertical, circular		
Antenna type	Omni, yagi element array, parabolic reflector, phased array		
Beam type – most common	Fan, pencil, cosecant squared		
Transmit and receive gain (dBi)		25.6	54
Elevation beamwidth (degrees)	Pencil beam	0.25	5.75
	Cosecant squared (CSC^2)	3.6 CSC^2 to 20	3.6 CSC^2 to 44
Azimuth beamwidth (degrees)	Pencil beam	0.4	5.75
Elevation scan angle limit (degrees)		–60	+90
Azimuth scan angle limit (degrees)		30 sector	360
First side-lobe level below main lobe peak (dB)		–35	–15.6

Table 1 was used to guide the development of the antenna types and patterns proposed.

2 Proposed formulae

In order to simplify the analysis, the antenna current distribution is considered as a function of either the elevation or azimuth coordinates. The directivity pattern, $F(\mu)$, of a given distribution is found from the finite Fourier transform as:

$$F(\mu) = \frac{1}{2}\int_{-1}^{+1} f(x) \cdot e^{j\mu x} dx$$

where:

$f(x)$: relative shape of field distribution, see Table 2 and Fig. 1

μ: provided in the table below = $\pi\left(\frac{l}{\lambda}\right)\sin(\alpha)$

l: overall length of aperture

λ: wavelength

ω: beam elevation or azimuth pointing (scan) angle

α: angle relative to aperture normal

θ: (α-ω) angle relative to aperture normal and pointing angle

x: normalized distance along aperture $-1 \leq x \leq 1$

j: complex number notation.

The proposed theoretical antenna patterns are provided in Table 2. The patterns are valid in the ±90° from beam scan angle relative to antenna boresight. Values more than ±90° from this angle are assumed to be in the back lobe where the antenna mask floor would apply. The parameters and formulae for determining antenna directivity patterns (ADP) that are presented in Table 2 (and thereafter in the related Table 3 and figures) are correct only in the case where the field amplitude at the edge of the antenna aperture is equal to zero and within the bounds of the main lobe and first two side lobes of the ADP. With other values of field amplitude at the edge of the antenna aperture, the form of the ADP and its parameters may differ significantly from the theoretical ones presented in this Recommendation. If real radar antenna patterns are available, then those should be digitized and used.

TABLE 2

Antenna directivity parameters

Relative shape of field distribution $f(x)$ where $-1 \le x \le 1$	**Directivity pattern $F(\mu)$**	**θ_3 half power beam-width (degrees)**	**μ as a function of θ_3**	**First side-lobe level below main lobe peak (dB)**	**Proposed mask floor level (dB)**	**Equation No.**
Uniform value of 1	$\frac{\sin(\mu)}{\mu}$	$50.8\left(\frac{\lambda}{l}\right)$	$\frac{\pi \cdot 50.8 \cdot \sin(\theta)}{\theta_3}$	−13.2	−30	(1)
COS(π*x/2)	$\frac{\pi}{2}\left[\frac{\cos(\mu)}{\left(\frac{\pi}{2}\right)^2 - \mu^2}\right]$	$68.8\left(\frac{\lambda}{l}\right)$	$\frac{\pi \cdot 68.8 \cdot \sin(\theta)}{\theta_3}$	−23	−50	(2)
COS(π*x/2)^2	$\frac{\pi^2}{2 \cdot \mu}\left[\frac{\sin(\mu)}{\left(\pi^2 - \mu^2\right)}\right]$	$83.2\left(\frac{\lambda}{l}\right)$	$\frac{\pi \cdot 83.2 \cdot \sin(\theta)}{\theta_3}$	−32	−60	(3)
COS(π*x/2)^3	$\frac{3 \cdot \pi \cdot \cos(\mu)}{8}\left[\frac{1}{\left(\frac{\pi}{2}\right)^2 - \mu^2} - \frac{1}{\left(\frac{3 \cdot \pi}{2}\right)^2 - \mu^2}\right]$	$95\left(\frac{\lambda}{l}\right)$	$\frac{\pi \cdot 95 \cdot \sin(\theta)}{\theta_3}$	−40	−70	(4)

where θ_3 is the 3 dB antenna half-power beamwidth (degrees). The relative shapes of the field distribution functions $f(x)$, as defined in Table 2, are plotted in Fig. 1.

FIGURE 1

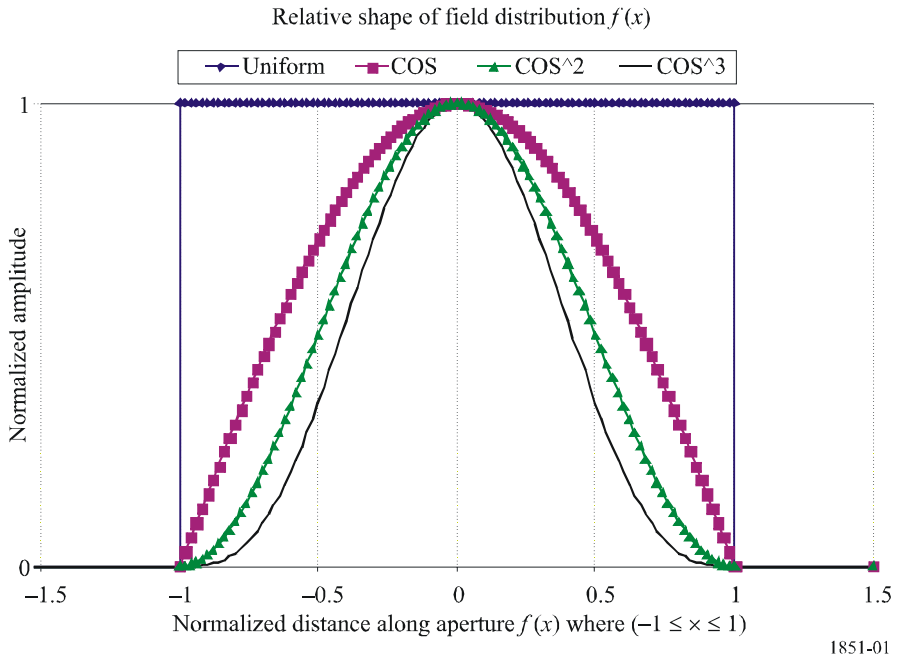

Given that the half power beamwidth, θ_3, is provided, the value of μ can be redefined as a function of the half-power antenna beamwidth. This is done by replacing the quantity $\left(\frac{l}{\lambda}\right)$ in $\mu = \pi\left(\frac{l}{\lambda}\right)\sin(\alpha)$ by a constant that depends on the relative shape of the field distribution; divided by the half-power beamwidth, θ_3, as shown in Table 2. These constant values of 50.8, 68.8, 83.2 and 95, shown in Table 2, can be derived by setting the equation for $F(\mu)$ equal to −3 dB, and solving for the angle θ.

Figure 2 shows the antenna patterns for cosine (COS), cosine-squared (COS^2) and cosine-cubed (COS^3) distribution functions.

FIGURE 2

Antenna pattern comparison, 3 dB beamwidth is 8.0°

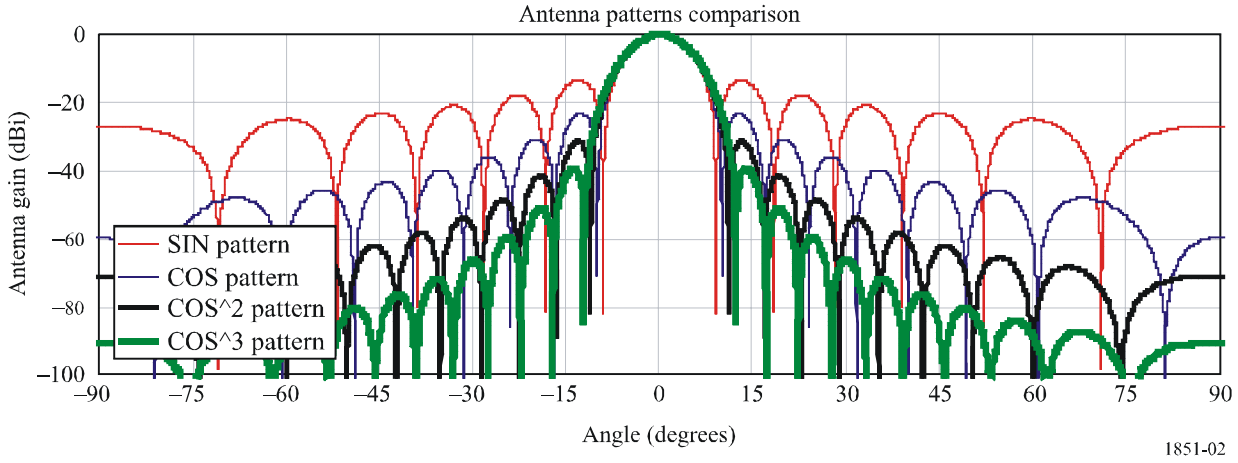

Using Fig. 2 above, the mask equations are derived by using a curve fit to the antenna peak side-lobe levels. It has been found, by comparing the integral of the theoretical and the proposed mask patterns, that the difference between the peak and average power in one principal plane cut is approximately 4 dB. The following definitions apply:

– convert equations (1) to (4) into dB using 20*log(abs(Directivity Pattern));

– normalize the antenna pattern gains. Uniform pattern does not require normalization, for cosine pattern subtract −3.92 dB, for cosine-squared pattern subtract −6.02 dB and for cosine-cubed pattern subtract −7.44 dB;

– to plot the mask, use the theoretical directivity pattern from Table 2, as shown in the previous two steps, up to the break point for either the peak or average antenna pattern, as required. After the break point, apply the mask pattern as indicated in Table 3;

– the peak pattern mask is the antenna pattern that rides over the side-lobe peaks. It is used for a single-entry interferer;

– the average pattern mask is the antenna pattern that approximates the integral value of the theoretical pattern. It is used for aggregated multiple interferers;

– the peak pattern mask break point is the point in pattern magnitude (dB) below the maximum gain where the pattern shape departs from the theoretical pattern into the peak mask pattern, as shown in Table 3;

– the average pattern mask break point is the point in pattern magnitude (dB) below the maximum gain where the pattern shape departs from the theoretical pattern into the average mask pattern, as shown in Table 3;

– θ_3 is the 3 dB antenna beamwidth (degrees);

– θ is the angle in either the elevation (vertical) or azimuth (horizontal) principal plane cuts (degrees);

– the average mask is the peak mask minus approximately 4 dB. Note that the break points of the peak pattern are different from the average patterns.

Table 3 shows the equations to be used in the calculations.

TABLE 3

Peak and average mask pattern equations

Pattern type	Mask equation beyond pattern break point where mask departs from theoretical pattern (dB)	Peak pattern break point where mask departs from theoretical pattern (dB)	Average pattern break point where mask departs from theoretical pattern (dB)	Constant added to the peak pattern to convert it to average mask (dB)	Equation No.
SIN	$-8.584 \cdot \ln\left(2.876 \cdot \frac{\lvert\theta\rvert}{\theta_3}\right)$	−5.75	−12.16	−3.72	(5)
COS	$-17.51 \cdot \ln\left(2.33 \cdot \frac{\lvert\theta\rvert}{\theta_3}\right)$	−14.4	−20.6	−4.32	(6)
COS^2	$-26.882 \cdot \ln\left(1.962 \cdot \frac{\lvert\theta\rvert}{\theta_3}\right)$	−22.3	−29.0	−4.6	(7)
COS^3	$-35.84 \cdot \ln\left(1.756 \cdot \frac{\lvert\theta\rvert}{\theta_3}\right)$	−31.5	−37.6	−4.2	(8)

The function ln() is the natural log function. An example of the break point is shown in Fig. 3.

FIGURE 3

Break point example

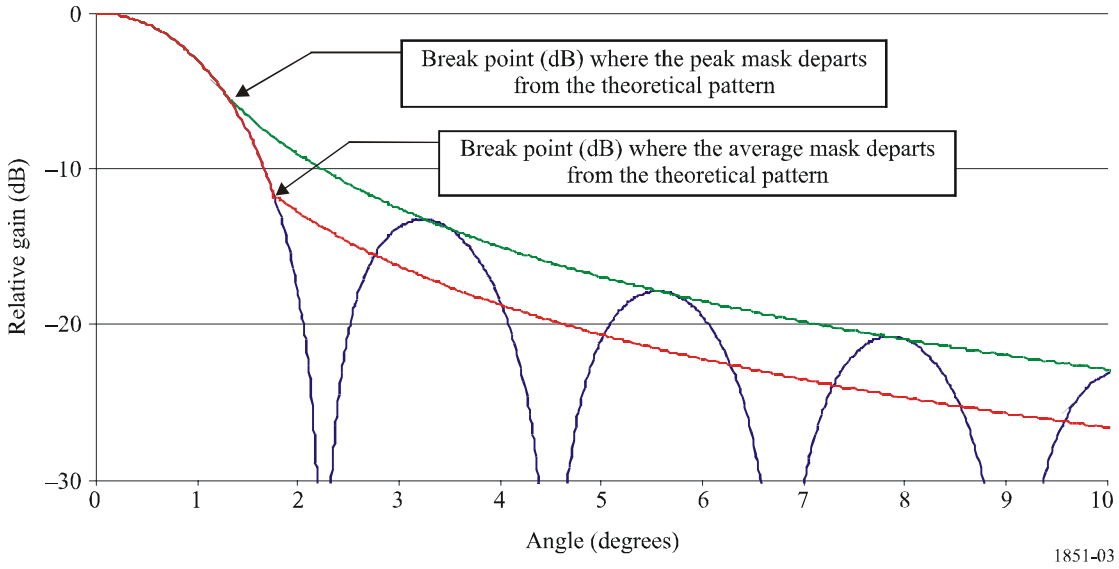

The cosecant-squared pattern is a special case. It is given by:

$$G(\theta) = G(\theta_1) \cdot \left(\frac{CSC(\theta)}{CSC(\theta_1)}\right)^2 \tag{9}$$

where:

$G(\theta)$: cosecant squared pattern between angles of θ_1 and θ_{Max}

$G(\theta_1)$: pattern gain at θ_1

θ_1: half power antenna beamwidth where cosecant-squared pattern starts = θ_3

θ_{Max}: maximum angle where cosecant-squared pattern stops

θ: elevation angle

θ_3: half power antenna beamwidth.

The average antenna pattern gain is not considered for the cosecant-squared pattern. It should be used for single and multiple interferers. The cosecant pattern is applied as follows:

TABLE 4

Cosecant-squared antenna pattern equations

Cosecant-squared equation	Condition	Equation No.
$\frac{\sin(\mu)}{\mu};\ \mu = (\pi \cdot 50.8 \cdot \sin(\theta))/\theta_3$	$\frac{-\theta_3}{0.88} \le \theta \le +\theta_3$	(10)
$G(\theta_1) \cdot \left(\frac{CSC(\theta)}{CSC(\theta_1)} \right)^2$	$+\theta_3 \le \theta \le \theta_{Max}$	(11)
Cosecant floor level (example = −55 dB)	$\theta_{Max} \le \theta \le \theta_{90}$	(12)
$G(\theta_1) = \frac{\sin\left(\frac{\pi \cdot 50.8 \cdot \sin(\theta_1)}{\theta_3} \right)}{\frac{\pi \cdot 50.8 \cdot \sin(\theta_1)}{\theta_3}}$	$\theta_1 = \theta_3$	(12a)

A graphical description of the patterns are shown in the figures below.

FIGURE 4

Cosecant squared beam coverage for search radar

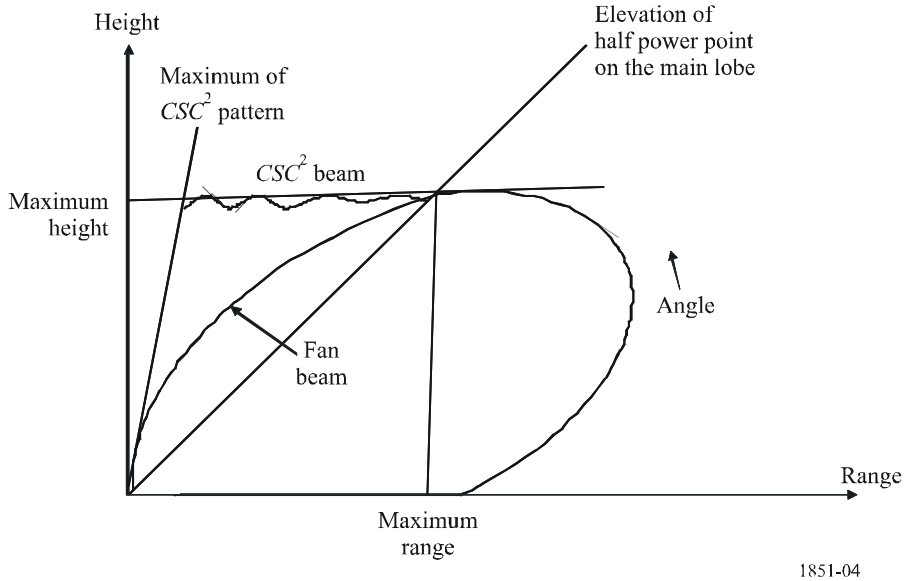

FIGURE 5

SIN antenna pattern, peak and average envelope

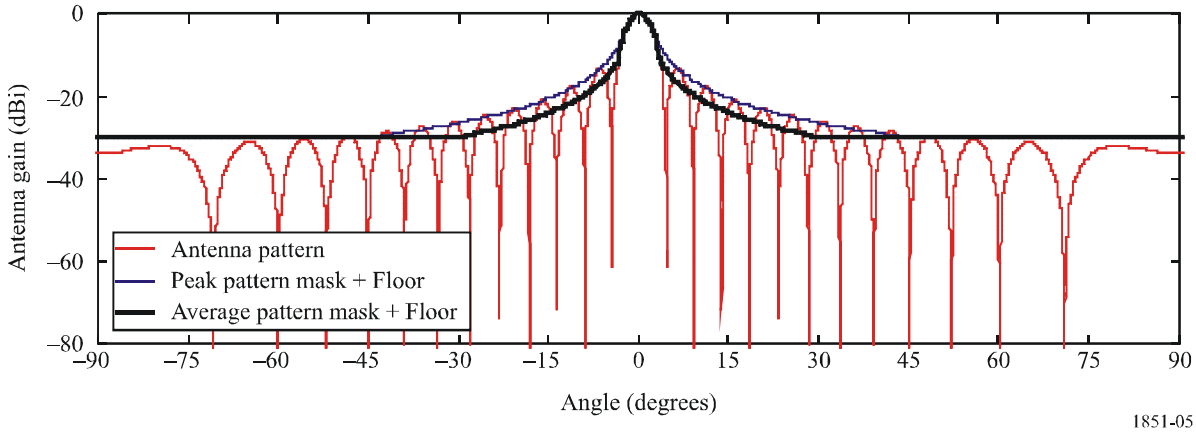

FIGURE 6

SIN polar antenna pattern, peak and average envelope

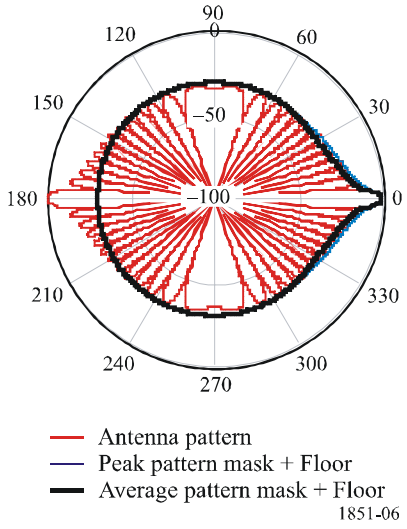

FIGURE 7

COS antenna pattern, peak and average envelope

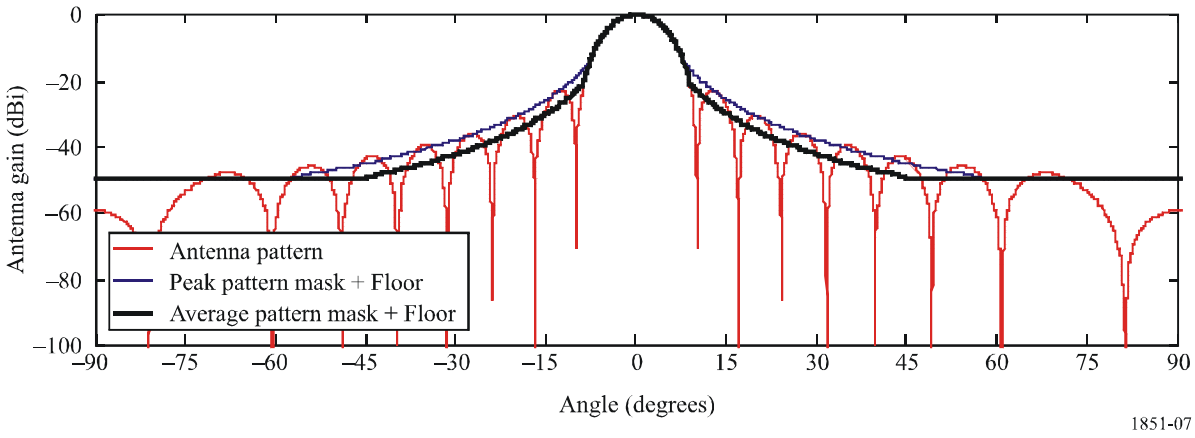

FIGURE 8

COS polar antenna pattern, peak and average envelope

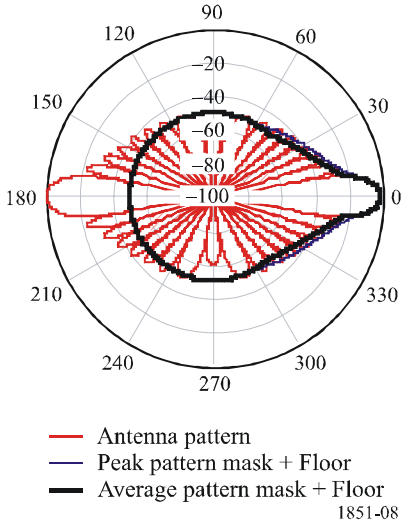

FIGURE 9

COS^2 antenna pattern, peak and average envelope

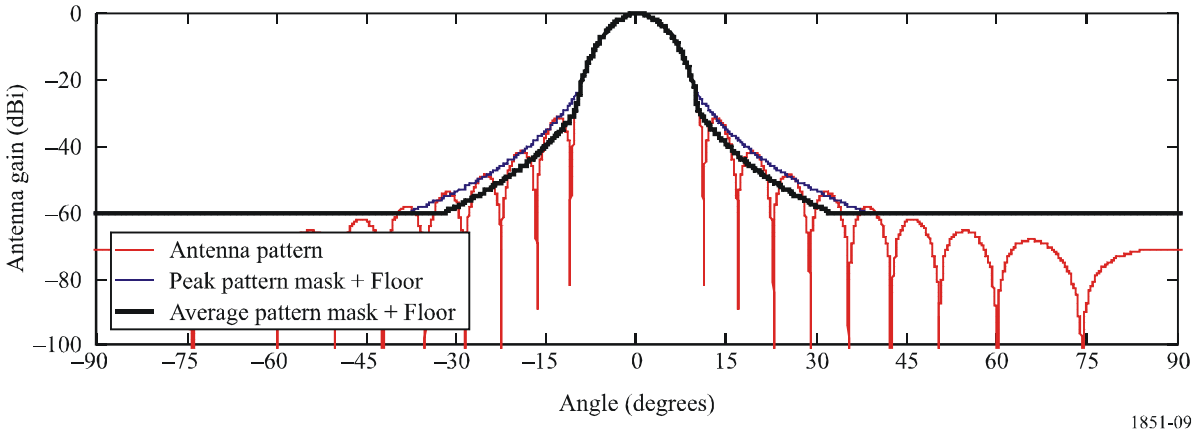

FIGURE 10

COS^2 polar antenna pattern, peak and average envelope

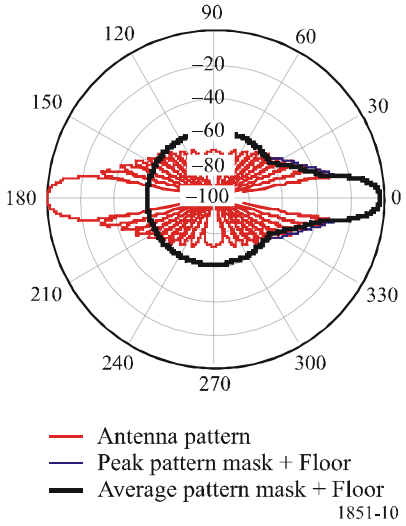

FIGURE 11

COS^3 antenna pattern, peak and average envelope

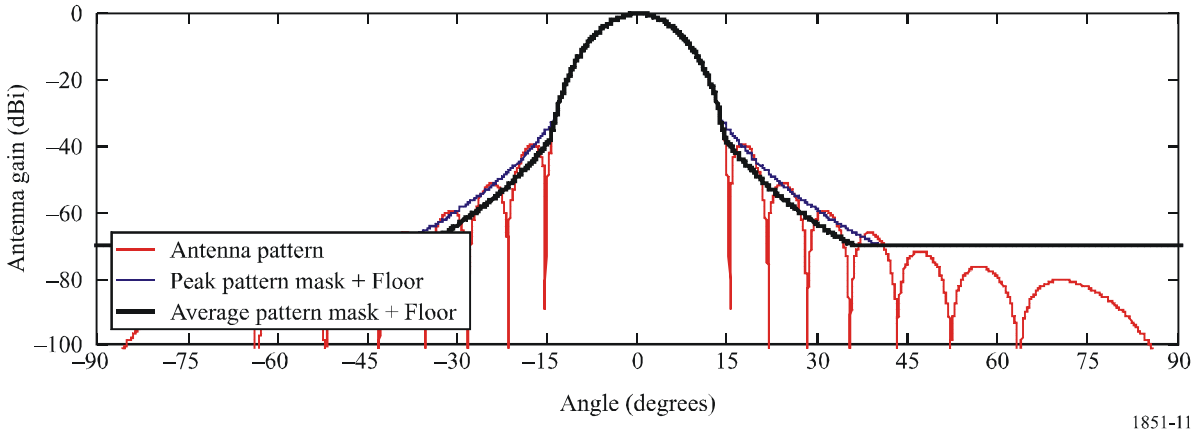

FIGURE 12

COS^3 polar antenna pattern, peak and average envelope

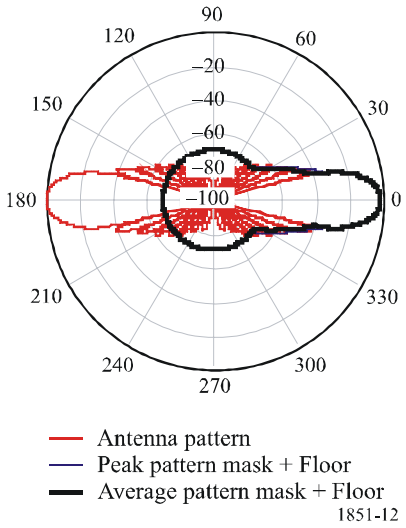

FIGURE 13

CSC^2 antenna pattern envelope

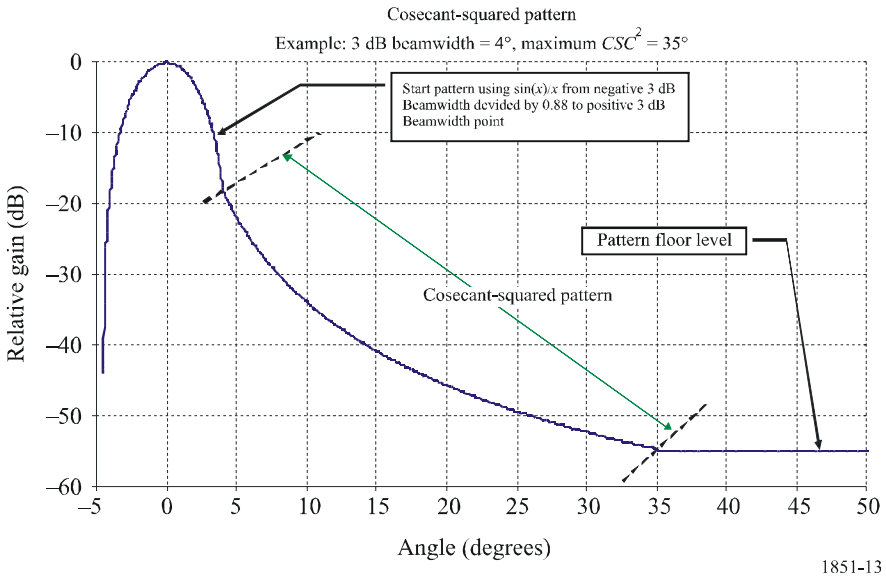

3 Antenna pattern selection

A suggestion for how the antenna pattern should be selected is based on information about half-power beamwidth and peak side-lobe level. This is provided in Table 5.

TABLE 5

Pattern selection table

Range of first side-lobe level below normalized main lobe peak (dB)	Possible antenna distribution type	Directivity pattern $F(\mu)$	Mask equation beyond pattern break point where mask varies from theoretical pattern (dB)	Peak pattern break point where mask varies from theoretical pattern (dB)	Average pattern break point where mask varies from theoretical pattern (dB)	Constant added to the peak pattern to convert it to average mask (dB)	Proposed mask floor level (dB)	Equation No.
−13.2 to −20 dB	Uniform	$\frac{\sin(\mu)}{\mu};\ \mu = (\pi \cdot 50.8 \cdot \sin(\theta))/\theta_3$	$-8.584 \cdot \ln\left(2.876 \cdot \frac{\lvert\theta\rvert}{\theta_3}\right)$	−5.75	−12.16	−3.72	−30	(13)
−20 to −30 dB	COS	$\frac{\pi}{2}\left[\frac{\cos(\mu)}{\left(\frac{\pi}{2}\right)^2 - \mu^2}\right];\ \mu = (\pi \cdot 68.8 \cdot \sin(\theta))/\theta_3$	$-17.51 \cdot \ln\left(2.33 \cdot \frac{\lvert\theta\rvert}{\theta_3}\right)$	−14.4	−20.6	−4.32	−50	(14)
−30 to −39 dB	COS^2	$\frac{\pi^2}{2 \cdot \mu}\left[\frac{\sin(\mu)}{\left(\pi^2 - \mu^2\right)}\right];\ \mu = (\pi \cdot 83.2 \cdot \sin(\theta))/\theta_3$	$-26.882 \cdot \ln\left(1.962 \cdot \frac{\lvert\theta\rvert}{\theta_3}\right)$	−22.3	−29.0	−4.6	−60	(15)
−39 dB or more	COS^3	$\frac{3 \cdot \pi \cdot \cos(\mu)}{8}\left[\frac{1}{\left(\frac{\pi}{2}\right)^2 - \mu^2} - \frac{1}{\left(\frac{3 \cdot \pi}{2}\right)^2 - \mu^2}\right];\ \mu = (\pi \cdot 95 \cdot \sin(\theta))/\theta_3$	$-35.84 \cdot \ln\left(1.756 \cdot \frac{\lvert\theta\rvert}{\theta_3}\right)$	−31.5	−37.6	−4.2	−70	(16)

4 Antenna pattern comparison

One mathematical model for radiodetermination radar antenna patterns that have been used in interference analysis is given in Recommendation ITU-R M.1652 includes equations for several patterns as a function of antenna gain. A comparison between the models developed in this Recommendation and Radar-C from Recommendation ITU-R M.1638 shows that the pattern in Recommendation ITU-R M.1652 is not optimal. As shown in Fig. 14, the pattern from Recommendation ITU-R M.1652 significantly overestimates the antenna gain off the antenna boresight (0°).

FIGURE 14

Antenna pattern comparison

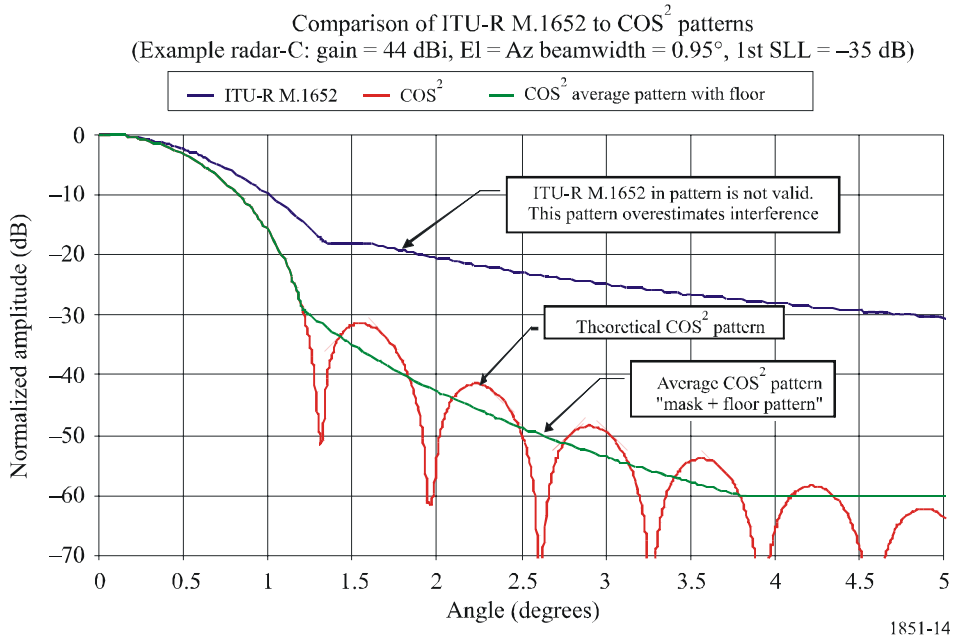

5 Approximating 3-dimensional (3-D) patterns

Data from the contour plots may be used as simulation analysis tools. The 3-dimensional (3-D) antenna pattern can easily be approximated. This is done by multiplying the horizontal and vertical principal plane voltage cuts. To do this, place the vertical principal plane pattern in the centre column of a square matrix, and set all the other elements to zero. Place the horizontal principal plane pattern in the centre row of a square matrix and set all the other elements to zero. Multiply the two matrices together and plot. Note that all patterns must be normalized.

The equation for calculating the 3-dimensional pattern is given by:

$$P_{i,h} = 20\log\left[\sum_{k=0}^{N}\left|H_{k,i}V_{h,k}\right|\right] \tag{17}$$

where the elevation and azimuth matrices, in units of volts, are defined in equations (18) and (19).

The vertical pattern is given by:

$$\text{Vertical matrix } (V_{h,k}) = \begin{vmatrix} 0 & .... & 0 & El_1 & 0 & .... & 0 \\ 0 & .... & 0 & El_2 & 0 & .... & 0 \\ .... & .... & 0 & El_3 & 0 & .... & .... \\ .... & .... & .... & .... & .... & .... & .... \\ .... & .... & .... & .... & .... & .... & .... \\ 0 & .... & 0 & El_{N-1} & 0 & .... & 0 \\ 0 & .... & 0 & El_N & 0 & .... & 0 \end{vmatrix} \quad (18)$$

The horizontal pattern is given by:

$$\text{Horizontal matrix } (H_{k,i}) = \begin{vmatrix} 0 & .... & .... & .... & .... & 0 \\ .... & .... & .... & .... & .... & .... \\ 0 & 0 & .... & .... & 0 & 0 \\ Az_1 & Az_2 & & & Az_{N-1} & Az_N \\ 0 & 0 & .... & .... & 0 & 0 \\ .... & .... & .... & .... & .... & .... \\ 0 & 0 & .... & .... & .... & 0 \end{vmatrix} \quad (19)$$

Figure 17 shows an example of a 3-dimensional pattern.

FIGURE 15

Antenna contour pattern for BW_H = 1.2° and BW_V = 6°

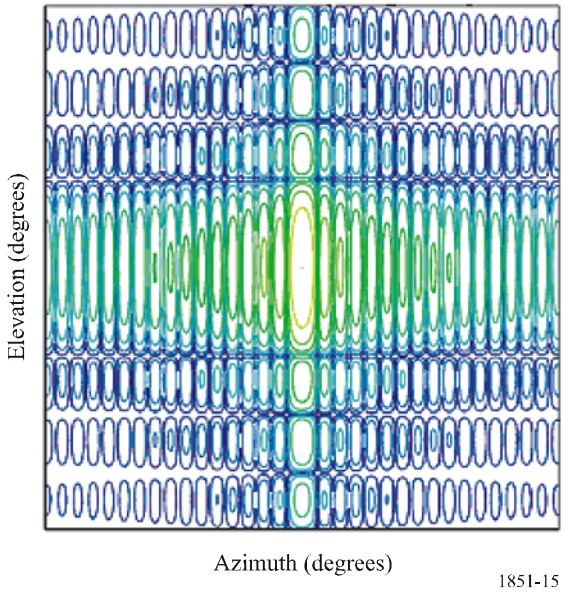

FIGURE 16

Antenna contour pattern for BW_H = BW_V = 1.7°

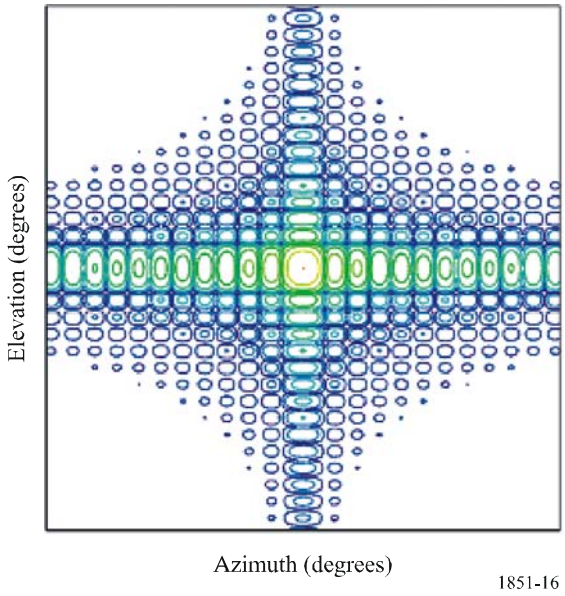

FIGURE 17

Example of a 3-dimensional antenna plot

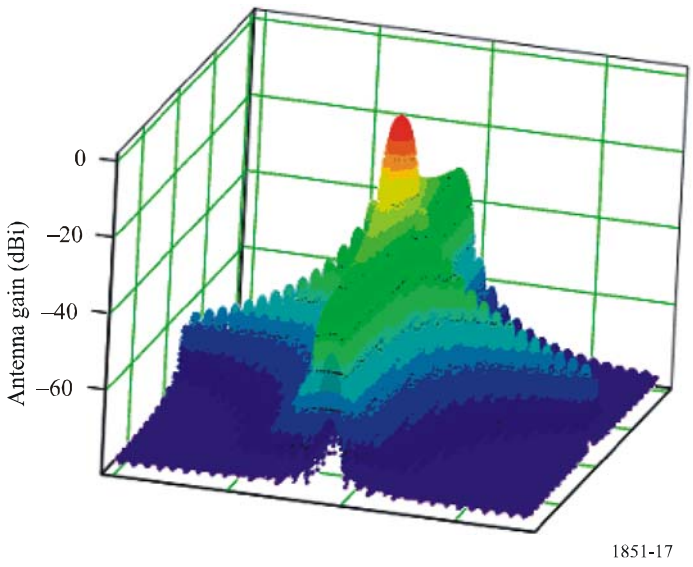

6 Measured pattern example

The following are examples of radar antenna pattern test data, in the 9 GHz band, that show the approximate peak side-lobe level and the pattern floor.

FIGURE 18

Example measured antenna plot

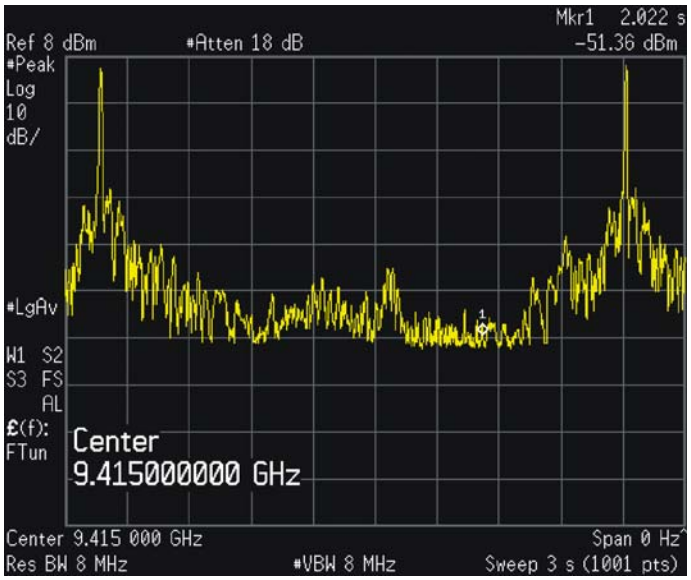

1851-18

FIGURE 19

Example measured antenna plot

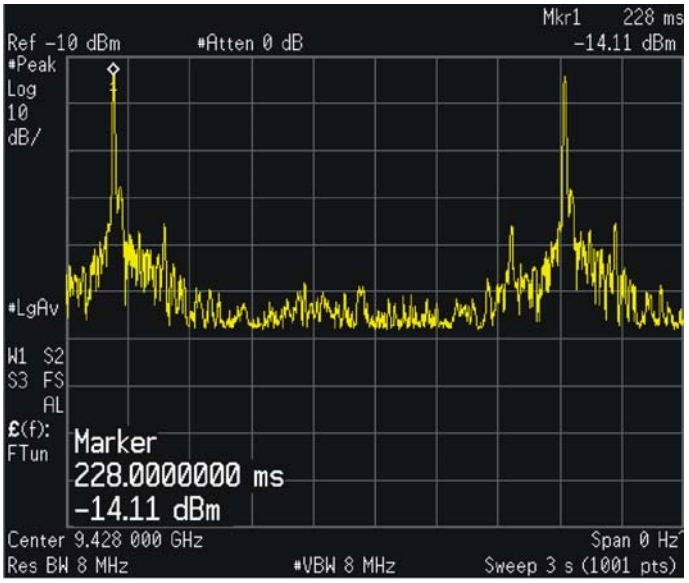

1851-19